Granular Matter (2012) 14:229–234
DOI 10.1007/s10035-012-0339-y

ORIGINAL PAPER

Surface curvature of steady granular flows

Jim N. McElwaine · Daisuke Takagi · Herbert E. Huppert

Received: 9 September 2011 / Published online: 18 March 2012

Abstract Laboratory experiments have shown that the steady flow of granular material down a rough inclined plane has a surface that is not parallel to the plane, but has a curvature across the slope with the height increasing toward the middle of the flow. We study this observation by postulating a new granular rheology, similar to that of a second order fluid. This model is applied to the experiments using a shallow water approximation, given that the depth of the flow is much smaller than the width. The model predicts that a second normal stress difference allows cross-slope height variations to develop in regions with considerable cross-slope velocity shear, consistent with the experiments. The model also predicts the development of lateral eddies, which are yet to be observed.

Keywords Shallow granular flow · Normal stress difference · Levée formation

1 Introduction

When a granular material is released steadily from a localised source down a rough plane inclined at a range of angles, a steady flow develops between static levées down the slope [1–3]. Remarkably, however, the surface of the flowing region is not parallel to the inclined plane, but is curved across the slope with the height decreasing from the middle toward the levées. Although the bulk region of the flow has little variation in height across the flow, variations in height and surface velocity arise particularly near the margins of the flow. To gain a better understanding of these experimental observations, we consider effects of normal stresses as a possible mechanism for the manifestation of the curved surface, as shown for non-Newtonian fluids flowing in a deep channel [4].

Many non-Newtonian fluids such as polymers exhibit normal stress differences [5]. This leads to the Weissenberg effect where a polymeric liquid will climb up a rotated rod. In particulate suspensions the second normal stress difference has the opposite sign and the surface will dip [6,7]. These systems were studied first by Bagnold [8] and the earlier experiments have recently been extended by Pouliquen [9], whose work provides a good summary of what is known. For purely granular systems there is little experimental data available [10], though it is clear from discrete element method simulations [11,12] that normal stress differences exist. For rapid flows, such differences are predicted theoretically by standard kinetic models [13,14] and have been observed experimentally [15]. For slow flows, simulations in a split-bottom shear geometry [16] indicate that second normal stress differences can be significant when first normal stress differences are zero, though the theory and experiments are less well understood. Normal stress differences are not incorporated in the widely used $\mu(I)$ model [17] of dense granular flows.

We propose a granular rheology that generalises the $\mu(I)$ model and incorporates first and second normal stress differences. A mathematical model is developed and applied to the experiments previously presented in detail in [3], which can be regarded as a granular channel flow. The model is consistent with the experimental observation that the height of the steady flow decreases from the middle of the flow particularly toward the margins, where the downslope velocity varies considerably in the cross-slope direction.

J. N. McElwaine (✉) · D. Takagi · H. E. Huppert
Department of Applied Mathematics and Theoretical Physics, Institute of Theoretical Geophysics, Centre for Mathematical Sciences, University of Cambridge, Wilberforce Road, Cambridge CB3 0WA, UK
e-mail: jnm11@cam.ac.uk

2 Theory

A general model for incompressible non-Newtonian fluids is the Rivlin-Ericksen nth-order fluid [18]. The classification comes from the school of rational mechanics [19]. This postulates that the stress tensor can be written in terms of the tensor quantities that can be calculated from the velocity field of the fluid. An ideal fluid, that is one without viscosity, is a zeroth order fluid; that is the stress tensor is independent of the velocity. A Newtonian fluid is a first order fluid; it is linear in derivatives of the velocity. Second order fluids are used to model non-spherical particles in suspension. They are a natural choice for granular materials since the second order terms are quadratic in derivatives of the velocities and this is the expected scaling for granular stresses on dimensional grounds.

Let $\mathbf{u}(\mathbf{r})$ be the fluid velocity as a function of position $\mathbf{r} = (r_1, r_2, r_3) = (x, y, z)$. We define $L_{ij} = \partial u_i/\partial r_i$, the strain tensor $A = L + L^T$ and the second Rivlin-Ericksen Tensor $B = \mathbf{u}\cdot\nabla A + L^T A + AL$. We consider a (steady) second order granular fluid to have the stress closure

$$\sigma = p\left[-\mathbf{1} + \mu\frac{A}{|A|} + (N_1 + N_2)\frac{A^2}{|A|^2} - \frac{1}{2}N_1\frac{B}{|A|^2}\right], \quad (1)$$

where $|A| = \sqrt{\mathrm{Tr}(A^2)/2}$ is the shear rate, μ the granular friction and N_1 and N_2 the non-dimensional first and second normal stress differences. This differs from the usual definition in the scaling with $|A|$ and all the coefficients are dimensionless.

This also needs an equation of state

$$p = d^2|A|^2\rho f(\phi), \quad (2)$$

where ρ is the bulk density and ϕ the packing fraction. In general f could also depend on the non-dimensional ratios of the tensor invariants of A. For example bulk friction (in analogy to bulk viscosity) could enter through $\mathrm{Tr}(A)/|A|$ if compressibility were important. Similarly μ, N_1 and N_2 can depend on these invariants and ϕ. This is the only way of writing a stress-strain relationship for a second order granular fluid that is dimensionally consistent and satisfies tensor invariance. Whenever the flow is close to local equilibrium and fields vary slowly such a form should be an accurate model. Close to boundaries other fields such as granular temperature are not slaved to the primary fields and must be included separately and more complicated constitutive laws are necessary. The approach by [17] is convenient for free surface flows and treats p as an independent variable. This is easily seen to be equivalent to the above formulation since $f = 1/I^2$ means that $\phi = f^{-1}(1/I^2)$ thus the functional dependence of μ on I can be replaced by a dependence of μ on ϕ. Note that with this definition $p \neq \mathrm{Tr}(\sigma)/3$ in general. The stress relation could be recast in this form however by redefining p and μ etc. μ, N_1 and N_2 are all functions of the non-dimensional group I which must therefore be constant up to $O(\epsilon^2)$, so it is only in the lowest order equations that their variation must be accounted for in determining $U(Z)$. Elsewhere they can be assumed to be constant except at $O(\epsilon^3)$ and higher.

We consider flow solutions on a flat slope of constant angle in the direction x. We make the ansatz that all quantities will vary slowly in the cross slope (z) direction and assume cross slope velocities will be of $O(\epsilon)$ and then, because of incompressibility, vertical velocities will be of $O(\epsilon^2)$. We define the slow horizontal variable $Z = \epsilon z$ and let the upper surface of the flow be $y = H(Z)$.

For a steady flow the kinematic free surface boundary condition is $\hat{\mathbf{n}}\cdot\mathbf{u}|_{s=0} = 0$ where $\hat{\mathbf{n}} \propto (0, 1, -\epsilon H_Z)$ and $s = (H - y)/H$. On the lower boundary we assume a no-slip boundary condition $\mathbf{u}|_{s=1} = 0$. The upper surface should satisfy a zero stress boundary condition $\hat{\mathbf{n}}\cdot\sigma|_{s=0} = 0$, but this is trivially satisfied for all components of σ if $p|_{s=0} = 0$ and μ, N_1 and N_2 are all finite, which we assume. The upper boundary is therefore a singularity of the pde where the order of the system drops. We instead assume a regularity condition, namely that all gradients of velocity remain finite. The Rivlin-Ericksen tensor B contains second order derivatives of u so that after taking derivatives of the stress tensor the system is third order in derivatives of $\mathbf{u}$ and three more boundary conditions should therefore be necessary. However, for the velocity fields that we will consider the system remains second order so we do not discuss this issue further. Momentum balance for steady flow is $\mathbf{u}\cdot\nabla\mathbf{u} = \nabla\sigma + \mathbf{g}$ and incompressibility $\nabla\cdot\mathbf{u} = 0$, which gives four equations. Using $\mathbf{u}(\mathbf{r}) = (u(y, Z), \epsilon^2 v(y, Z), \epsilon w(y, Z))$ then accurate to $O(\epsilon^2)$, we obtain

$$A = \begin{pmatrix} 0 & u_y & \epsilon u_Z \\ u_y & 2\epsilon^2 v_y & \epsilon w_y \\ \epsilon u_Z & \epsilon w_y & 2\epsilon^2 w_Z \end{pmatrix}, \quad (3)$$

$$A^2 = \begin{pmatrix} u_y^2 + \epsilon^2 u_Z^2 & 2\epsilon^2 u_y v_y + \epsilon^2 u_Z w_y & \epsilon u_y w_y \\ 2\epsilon^2 u_y v_y + \epsilon^2 u_Z w_y & u_y^2 + \epsilon^2 w_y^2 & \epsilon u_y u_Z \\ \epsilon u_y w_y & \epsilon u_y u_Z & \epsilon^2 u_Z^2 + \epsilon^2 w_y^2 \end{pmatrix},$$

$$|A|^2 = u_y^2 + \epsilon^2 u_Z^2 + \epsilon^2 w_y^2. \quad (4)$$

From this it is clear that in simple shear

$$A^2/|A|^2 = \begin{pmatrix} 1 & 0 & 0 \\ 0 & 1 & 0 \\ 0 & 0 & 0 \end{pmatrix},$$

thus setting the second normal stress difference. This shows that our model with $N_1 = 0$ is a generalisation of that in [16] written in tensorial form.

We will assume that u_y is always positive and large enough compared to u_Z and w_y so that

$$|A| = u_y + \frac{\epsilon^2}{2}\frac{u_Z^2 + w_y^2}{u_y}. \tag{5}$$

The non-zero components of B are then

$$\begin{aligned} B_{xy} &= \epsilon^2(v u_{yy} + w u_{yZ} + v_y u_y + u_Z w_y),\\ B_{yy} &= 2u_y^2 + 2\epsilon^2 w_y^2,\\ B_{yz} &= 2\epsilon u_y u_Z,\\ B_{zz} &= 2\epsilon^2 u_Z^2, \end{aligned} \tag{6}$$

explaining our choice of N_1 and N_2 in Eq. 1.

The stress components accurate to $O(\epsilon^2)$ are then

$$\begin{aligned} \frac{\sigma_{xx}}{p} &= -1 + N_1 + N_2 - \epsilon^2(N_1+N_2)\frac{w_y^2}{u_y^2},\\ \frac{\sigma_{yy}}{p} &= -1 + N_2 + \epsilon^2 2\mu\frac{v_y}{u_y} - \epsilon^2 N_2\frac{u_Z^2}{u_y^2},\\ \frac{\sigma_{zz}}{p} &= -1 + 2\epsilon^2\mu\frac{w_Z}{u_y} + \epsilon^2(N_1+N_2)\frac{w_y^2}{u_y^2} + \epsilon^2 N_2\frac{u_Z^2}{u_y^2},\\ \frac{\sigma_{xy}}{p} &= \mu + \frac{\epsilon^2}{2}(3N_1+4N_2)\frac{v_y}{u_y}\\ &\quad + \frac{\epsilon^2}{2}\left[(N_1+2N_2)\frac{u_Z w_y}{u_y^2} - \mu\frac{u_Z^2+w_y^2}{u_y^2} - N_1\frac{v u_{yy} + w u_{yZ}}{u_y^2}\right],\\ \frac{\sigma_{yz}}{p} &= \epsilon\mu\frac{w_y}{u_y} + \epsilon N_2\frac{u_Z}{u_y},\\ \frac{\sigma_{xz}}{p} &= \epsilon(N_1+N_2)\frac{w_y}{u_y} + \epsilon\mu\frac{u_Z}{u_y},\\ \frac{\mathrm{Tr}\,\sigma}{p} &= -3 + N_1 + 2N_2 + 2\epsilon^2\mu\frac{v_y + w_Z}{u_y}\\ &= -3 + N_1 + 2N_2. \end{aligned}$$

This last simplification for $\mathrm{Tr}(\sigma)/p$ follows from incompressibility. The normal stress differences are then

$$\begin{aligned} \sigma_{xx} - \sigma_{yy} &= pN_1 + O(\epsilon^2),\\ \sigma_{yy} - \sigma_{zz} &= pN_2 + O(\epsilon^2). \end{aligned}$$

Using incompressibility, $v_y = -w_Z$, in the y momentum balance, we obtain

$$\left[-p(1-N_2) - p\epsilon^2\left(2\mu\frac{w_Z}{u_y} + N_2\frac{u_Z^2}{u_y^2}\right)\right]_y \tag{7}$$

$$+\epsilon^2\left[p\mu\frac{w_y}{u_y} + pN_2\frac{u_Z}{u_y}\right]_Z = g_y, \tag{8}$$

$$p_y(y = H(Z), Z)) = 0, \tag{9}$$

where the subscripts $[]_y$ and $[]_Z$ denote partial derivatives. The order of the σ_{yz} term has changed from ϵ to ϵ^2 as the derivative is now written with respect to Z. This is solved, accurate to $O(\epsilon^2)$, as

$$\begin{aligned} \frac{p}{g_y} &= \frac{H-y}{1-N_2} - \epsilon^2\frac{H-y}{(1-N_2)^2}\left(2\mu\frac{w_Z}{u_y} + N_2\frac{u_Z^2}{u_y^2}\right)\\ &\quad + \epsilon^2\int_y^H\left[\frac{H-y}{(1-N_2)^2}\left(\mu\frac{w_y}{u_y} + N_2\frac{u_Z}{u_y}\right)\right]_Z dy. \end{aligned} \tag{10}$$

In the z momentum equation we only need σ_{zz} accurate to $O(\epsilon)$ because we take the derivative with respect to z and this is now simply

$$\sigma_{zz} = -g_y\frac{H-y}{1-N_2}. \tag{11}$$

The z momentum equation is therefore

$$\left[-g_y\frac{H-y}{1-N_2}\right]_Z + g_y\left[\frac{H-y}{1-N_2}\left(\mu\frac{w_y}{u_y} + N_2\frac{u_Z}{u_y}\right)\right]_y = 0. \tag{12}$$

If we integrate this with respect to y and multiply by $(1-N_2)/g_y$ then

$$(H-y)\left(H_Z + \mu\frac{w_y}{u_y} + N_2\frac{u_Z}{u_y}\right) + C(Z) = 0, \tag{13}$$

where $C(Z)$ is an arbitrary function of Z. This can be rewritten

$$\mu w_y = -u_y H_Z - N_2 u_Z - \frac{u_y}{H-y}C(Z). \tag{14}$$

This shows that horizontal velocities are driven by gradients in downslope velocity if N_2 is non-zero, and by gradients in the surface height H_Z. Because the system is singular on the upper surface, all components of σ are 0 and the equation drops order and we do not have a boundary condition to apply. However, a reasonable physical condition is that all velocity gradients are finite. u_y near the surface of a granular flow typically behaves as $(H-y)^{1/2}$ or some lower power. w_Z and u_Z will only be finite if $C(Z) = 0$. Integrating this equation from the basal surface $y = 0$ where $w = 0, u = 0$, we obtain

$$\mu w = -uH_Z - N_2\int_0^y u_Z\,dy = -uH_Z - N_2\left[\int_0^y u\,dy\right]_Z. \tag{15}$$

Thus we see clearly that surface height gradients drive horizontal velocities and also horizontal velocity gradients through the second normal stress difference. Finally we must impose the surface kinematic boundary condition $v|_{y=H} = H_Z w|_{y=H}$. Using incompressibility we see that

$$v|_{y=H} = -\int_0^H w_Z \, dy = -\left[\int_0^H w \, dy\right]_Z + H_Z w|_{y=H}. \quad (16)$$

Since $w|_{y=0} = 0$ the kinematic condition is equivalent to

$$\left[\int_0^H w \, dy\right]_Z = 0,$$

that is the total cross flow is constant. In experiments with levées or side walls the constant will always be zero so the final condition on w is

$$0 = \int_0^H w \, dy = \int_0^H \left[uH_Z + N_2 \int_0^y u_Z \, dy\right] dy$$
$$= \int_0^H \left[uH_Z + N_2(H-y)u_Z\right] dy. \quad (17)$$

Equation 15 expresses a local balance between driving forces and the resulting flux w, but the steady flow w is only set by imposing the global constraint equation 17. To use this equation we must know the vertical velocity profile $u(y, Z)$. There is considerable experimental and numerical evidence that the velocity in a granular flow has a power law profile, so we assume

$$u = U(Z)\left(1 - s^\alpha\right), \quad (18)$$

where $s = 1 - y/H$. Thus $s = 0$ on the free surface and $s = 1$ on the basal surface. A Bagnold profile would be $\alpha = 3/2$, but shallow flows are generally linear, $\alpha = 1$ or even $\alpha < 1$. A complete theory would predict this, but this is beyond the scope of this paper. The solution for w from Eq. 15 is then

$$\mu w = -(1-N_2)(1-s^\alpha)UH_Z \quad (19)$$
$$- \frac{N_2}{1+\alpha}\left[\alpha(1-s)(HU)_Z - s(1-s^\alpha)(HU_Z - \alpha U H_Z)\right].$$

Integrating this with respect to s between 0 and 1 to impose the constraint 17 then solving for H_Z, we obtain

$$\frac{H_Z}{H} = -\frac{N_2}{2}\frac{1+\alpha}{2+\alpha-N_2}\frac{U_Z}{U} = \lambda\frac{U_Z}{U}, \quad (20)$$

where we have defined $\lambda = -\frac{1}{2}N_2(1+\alpha)/(2+\alpha-N_2)$. This shows that the deformations of the top surface is proportional to the surface strain rate U_Z. Equation 20 is easily solved to give H as a function of U

$$H/H_0 = (U/U_0)^\lambda, \quad (21)$$

where H_0 and U_0 are constants of integration.

This variation in surface height will result in a flow on the surface, which must be balanced by internal cross slope eddies. Evaluating w on the surface $s = 0$, we obtain

$$\mu w|_{s=0} = -(1-N_2)UH_Z - N_2\frac{\alpha}{1+\alpha}\partial_Z(UH)$$
$$= -\frac{N_2}{2}HU_Z\left(\frac{1}{2+\alpha-N_2} + \frac{\alpha-1}{\alpha+1}\right), \quad (22)$$

where we have used Eq. 20 to eliminate H_Z. These two equations clearly show the forcing induced by U_Z on H and w.

The Eq. 20 comes from y and z momentum balance assuming cross-slope variations are small and down-slope variations are zero. The remaining equation to solve is a down-slope momentum balance equation. However, despite recent theoretical developments [17] there are no straightforward theories that are applicable for flows close to jamming [20,21]. Instead in this paper we concentrate on the variation of H as a function of U, where U is measured in the experiments, which we discuss in the next section.

3 Laboratory experiments

We carried out a series of laboratory experiments to investigate the flow of granular material from a localised source on a rough inclined plane (described in more detail in [3]). The experimental set up is shown in Fig. 1. A cylindrical, perspex hopper of diameter 250 mm and height 700 mm was filled with the granular material. The experiments were performed with angular sand grains of size 0.45 ± 0.15 mm. The bottom of the hopper was connected to a cone which fed the grains into a smooth pipe of diameter 30 mm. A control valve across the pipe allowed the mass flow rate Q to be set to 0 or controlled between 5 and 218 $\mathrm{g\,s^{-1}}$, with a repeatability better than ± 2 $\mathrm{g\,s^{-1}}$. Below the control valve the grains fell freely down a tube onto a block of foam, which was highly inelastic and absorbed the energy of the impacting grains on the inclined plane. There was a 'V'-shaped groove cut into the middle of the foam to produce a localised source of dense granular flow.

The grains flowed down an inclined plane of length 3 m and width 1 m, wider than any of the flows in the experiments. The plane was made rough by gluing the same sand on the surface. Before each experimental run, the plane was covered in an erodible layer of uniform thickness H_{stop}. This configuration allows the system to approach any long-time state more quickly than an inclined plane initially free of grains (see Fig. 2). The erodible layer was set up by releasing a large flux of grains and then abruptly stopping the flow, a technique adopted previously [22]. All the results in this paper were performed on a slope of 32° to the horizontal which is just above the minimum angle for steady flow. At higher angles steady flows were hard to achieve because roll waves develop while at lower angles discrete avalanches occur at lower mass flow rates [3]. The flows in the experiments could be maintained indefinitely by transferring the grains that flowed off

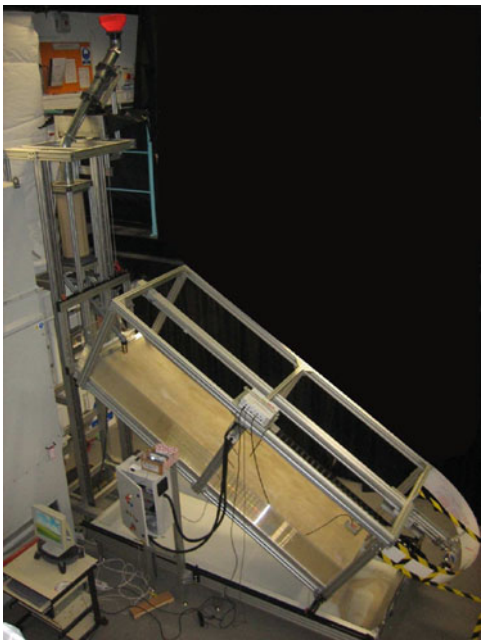

Fig. 1 Photograph shows the experimental set up. The cylindrical hopper of sand, the rough inclined plane and the instruments used to measure the flow are all supported by an aluminium framework

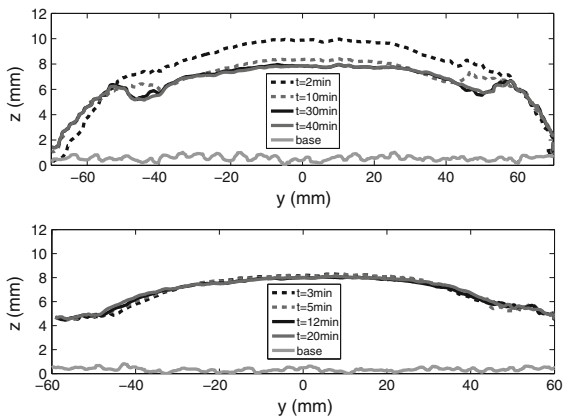

Fig. 2 Thickness of sand at different times for $50\,\mathrm{g\,s^{-1}}$. The *upper panel* shows the results when the surface is initially free of sand, whereas the *lower panel* shows the case when the lower panel was initially covered in sand. The value of H_{stop} is 4.5 mm

the inclined plane back into the hopper. Experiments were continues for up to 90 min to ensure that steady state was achieved.

The thickness and surface velocity of the flows were measured 2 m down the slope where the flows were steady and no longer depended on the x position. The thickness profile was measured to an accuracy of ± 0.1 mm at 1 kHz over a region of length $\approx$ 130 mm using a laser triangulator (Micro-Epsilon LLT2800–100 2D Laser displacement measuring system). The instrument was mounted on a linear traverse system to verify that steady flows are uniform down

Fig. 3 Photograph shows steady levées with slight slope curvature

the inclined plane. For steady flows of width greater than 130 mm (the widest flows were 250 mm), the instrument was positioned to observe either one edge or the centre of the whole flow. Surface velocities were measured to an accuracy of $\pm 0.3\,\mathrm{mm\,s^{-1}}$ with a high-speed camera (Photron SA1 5 400 fps, $1,024 \times 1,024$ pixels, 12 bit ADC) using PIV [23]. The cross-stream thickness and velocity profiles of steady flows were averaged over 30 seconds to reduce statistical fluctuations. A typical steady flow is shown in Fig. 3.

Figure 4 shows the steady height and velocity profiles for 6 experiments with mass flow rates 31, 50, 75, 104, 139 and $218\,\mathrm{g\,s^{-1}}$. The cross slope curvature is clearly visible in all the experiments. The lower panel shows the corresponding velocities. Since H increases with U this means that N_2, the second normal stress difference, is negative. Figure 5 shows H as a function of U. Equation 21 predicts that this should be a power law relationship. However our analysis is based on horizontal shear being small compared to vertical shear which requires $|U_z| \ll U/Z$. This is true in the centre but in the margins $U \to 0$, while $H \to H_{\mathrm{stop}}$ and U_z is non-zero so our assumption is invalid. This means that we only expect agreement when U is reasonably large. Near the margins the flow must be fully 2-dimensional and a depth integrated model is inapplicable in the form we have presented here. Nevertheless, the data in Fig. 5 do show a collapse onto a single curve, but not a power law since H does not go to 0 at $U = 0$. The collapse does suggest that there is a a one-to-one relation between H and U and thus it may be possible for a depth integrated theory to match the data. If we allow a generalised power law

$$(H - H_1)/H_0 = (U/U_0)^{\lambda}\,, \tag{23}$$

where the offset H_1 is a little larger than H_{stop}, then we do get reasonable agreement with $\lambda = 1$ except for the smallest U. We have no explanation for this at present, but note that granular flow rules also exhibit this problem.

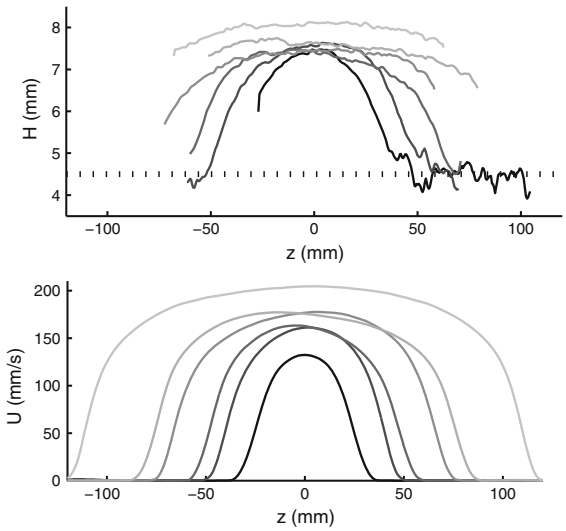

Fig. 4 *Upper* Cross slope height profiles for different mass flow rates with the *dashed line* showing H_{stop}. *Lower* Cross slope velocity profiles for the same experiments

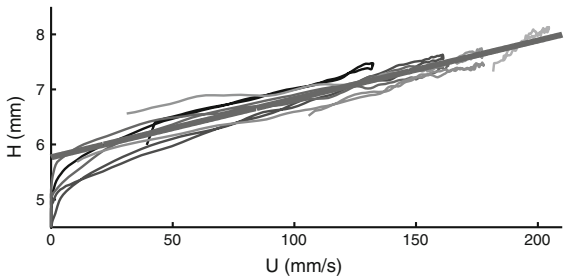

Fig. 5 Height profile as a function of surface velocity. The *thick grey line* is the best linear fit

For negative N_2 Eq. 22 predicts surface velocities towards regions of higher velocity. Figure 4 shows that an order of magnitude estimate for HU_Z is 5 mm s^{-1}. This is around 1/30 of the down-slope surface velocities and is not easily measured using PIV. Future experiments using particle tracking might better be able to confirm the existence of these eddies.

This paper has shown that shallow granular flows develop curved surfaces and that this can be explained by modelling them as a second order fluid. We have developed a depth averaged theory valid when cross-slope gradients are small, but this theory is inapplicable near the static levées, where the largest velocity and height gradients occur. This may explain why the height-velocity relation is not a power law as predicted by this theory.

We dedicate this paper to the memory of Isaac Goldhirsch, scholar, colleague and friend, who enriched our lives with many of his shared thoughts and conversations.

Acknowledgments The experimental apparatus was constructed by John Milton, David Page-Croft, Trevor Parkin and Neil Price. DT was funded by a Gates Cambridge Scholarship, JNM is an EPSRC Advanced Research Fellow and HEH is partially supported by a Royal Society Wolfson Research Merit Award. The authors would like to thank Nathalie Vriend for helpful discussions.

References

1. Felix, G., Thomas, N.: Relation between dry granular flow regimes and morphology of deposits: formation of levees in pyroclastic deposits. Earth Planet Sci. Lett. **221**, 197 (2004)
2. Deboeuf, S., Lajeunesse, E., Dauchot, O., Andreotti, B.: Flow rule, self-channelization, and levees in unconfined granular flows. Phys. Rev. Lett. **97**, 158303 (2006)
3. Takagi, D., McElwaine, J.N., Huppert, H.H.: Shallow granular flows. Phys. Rev. E **83**, 031306 (2011)
4. Tanner, R.I.: Some methods for estimating the normal stress functions in viscometric flows. J. Rheol. **14**, 483–507 (1970)
5. Bird, R.B., Armstrong, R.C., Hassager, O.: Dynamics of Polymeric Liquids. 2 edn. Volume 1. Wiley, (1987)
6. Singh, A., R.Nott, P.: Experimental measurements of the normal stresses in sheared stokesian suspensions. J. Fluid Mech. **490**, 293–320 (2003)
7. Zarraga, I.E., Hill, D.A., Leighton, D.T.: The characterization of the total stress of concentrated suspensions of noncolloidal spheres in newtonian fluids. J. Rheol. **44**, 185 (2000)
8. Bagnold, R.A.: Experiments on a gravity-free dispersion of large solid spheres in a newtonian fluid under shear. Proc. R. Soc. Lond. A Math. Phys. Sci. **225**, 49–63 (1954)
9. Boyer, F., Pouliquen, O., Guazzelli, E.: Dense suspensions in rotating-rod flows: normal stresses and particle migration. J. Fluid Mech. **686**, 5–25 (2011)
10. Campbell, C.S.: Rapid granular flows. Annu. Rev. Fluid Mech. **22**, 57–92 (1990)
11. Silbert, L.E., Ertaz, D., Grest, G.S., Halsey, T.C., Levine, D., Plimpton, S.J.: Granular flow down an inclined plane: Bagnold scaling and rheology. Phys. Rev. E **64**, 051302 (2001)
12. Börzsönyi, T., Ecke, R.E., McElwaine, J.N.: Patterns in flowing sand: understanding the physics of granular flow. Phys. Rev. Lett. **103**, 178302 (2009)
13. Goldhirsch, I., Sela, N.: Origin of normal stress differences in rapid granular flows. Phys. Rev. E **54**, 4458–4461 (1996)
14. Goldhirsch, I.: Rapid granular flows. Annu. Rev. Fluid Mech. **35**, 267–293 (2003)
15. McElwaine, J.N., Nishimura, K.: Ping-pong ball avalanche experiments. Ann. Glaciol. **32**, 241–250 (2001)
16. Depken, M., Lechman, J.B., Hecke, M.van , Saarloos, W. van , Grest, G.S.: Stresses in smooth flows of dense granular media. EPL (Europhys. Lett.) **78**, 58001 (2007)
17. Jop, P., Forterre, Y., Pouliquen, O.: A constitutive law for dense granular flows. Nature **441**, 727 (2006)
18. Leal, L.G.: The slow motion of slender rod-like particles in a second-order fluid. J. Fluid Mech. **69**, 305–337 (1975)
19. Truesdell, C.A.: A First Course in Rational Continuum Mechanics. Academic Press, New York (1977)
20. Rajchenbach, J.: Dense, rapid flows of inelastic grains under gravity. Phys. Rev. Lett. **90**, 144302 (2003)
21. Pouliquen, O., Forterre, Y.: A non-local rheology for dense granular flows. Philos. Trans. R. Soc. A Math. Phys. Eng. Sci. **367**, 5091 (2009)
22. Pouliquen, O.: Scaling laws in granular flows down rough inclined planes. Phys. Fluids **11**, 542 (1999)
23. Dalziel, S.B.: Digiflow, dl research partners, version 0.7 (2003)